(D) C/EBP:ATF composite sites in intron 1 of the *Eif4ebp1* gene. Mouse, rat and human *Eif4ebp1* gene segments are aligned with ATF4 binding sequences in several genes. Numbers are positions relative to A of the initial ATG codon. *Asns*, asparagine synthetase.

(E) A ChIP assay of MIN6 cells treated with Tg. DNAs precipitated with non-specific or anti-ATF4 IgG were amplified using primers for the *Eif4ebp1* intron 1 region.

(F) ATF4 induction of luciferase reporters with the *SV40* promoter and an *Eif4ebp1* gene segment with C/EBP:ATF composite sites or their mutants shown in (D). MIN6 cells were transfected with luciferase reporters together with either pCMV-empty or pCMV-ATF4. Error bars represent SEM. n = 4; *P < 0.05, **P < 0.01.

Figure 3. 4E-BP1-deficient cells exhibit increased apoptosis susceptibility with deregulated translational control

(A) Viability of MIN6*WT* and MIN6*Eif4ebp1*$^{-/-}$ cells treated with 0.5 μM thapsigargin (Tg) or 1.0 μg/ml tunicamycin (Tm) for 36 hr. Data from MIN6*WT* cells treated with vehicle (0.05% DMSO) were taken as 100%. n = 3-4. *P < 0.05; **P < 0.01.

(B) Immunoblot of cleaved caspase 3 in MIN6*WT* and MIN6*Eif4ebp1*$^{-/-}$ cells treated with vehicle control (Con) or Tg for 24 hr.

(C) Immunoblot analysis of 4EBP1, 4E-BP2, eIF4E and eIF4G in whole cell lysates (left) or in a complex associated with ^{7}mGTP-Sepharose (right) in cells treated with Tg for 24 hr.

(D) [^{35}S]methionine/cysteine incorporation during a 15-min pulse-label in MIN6*WT* and MIN6*Eif4ebp1*$^{-/-}$ cells pre-treated with Tg for indicated periods. Ten % of lysates were also probed with an anti-actin antibody. A representative autoradiogram is shown in the

upper panel. Data from 3 experiments are summarized in the lower panel.

(E) Greater CHOP induction in MIN6*Eif4ebp1*$^{-/-}$ cells treated with Tg. Representative blots are shown in the upper panel, data from 4 experiments are summarized in the lower panel.

(F) *Chop* mRNA levels in MIN6*WT* and MIN6*Eif4ebp1*$^{-/-}$ cells treated with Tg.

(G) Greater *Chop* translation in MIN6*Eif4ebp1*$^{-/-}$ cells treated with Tg. MIN6*WT* and MIN6*Eif4ebp1*$^{-/-}$ cells treated with vehicle (C) or Tg for 12 hr were labeled with [^{35}S]Met/Cys. Lysates were either directly subjected to SDS-PAGE or immunoprecipitated with anti-CHOP antibody. Representative autoradiograms are shown in the left. Data from 4 experiments are summarized in the right.

Error bars represent SEM. *P < 0.05. **P < 0.01.

Figure 4. β cell loss is exacerbated by 4E-BP1 deficiency in mouse diabetes models

(A) Fed blood glucose levels of wild-type (n = 6), *Eif4ebp1*$^{-/-}$ (n = 5), *Ins2*$^{WT/C96Y}$ (n = 9) and *Eif4ebp1*$^{-/-}$*Ins2*$^{WT/C96Y}$ (n = 11) mice. Data from three cohorts are combined. *P < 0.05, **P < 0.01 vs. *Ins2*$^{WT/C96Y}$ mice.

(B) Fed blood glucose levels of wild-type (*n* = 12), *Eif4ebp1*$^{-/-}$ (n = 8), *Wfs1*$^{-/-}$ (n = 15) and *Eif4ebp1*$^{-/-}$*Wfs1*$^{-/-}$ (n = 10) mice. Data from three cohorts are combined. *P < 0.05, **P < 0.01 vs. wild-type mice. ##P < 0.01 vs. *Wfs1*$^{-/-}$ mice.

(C) Pancreatic insulin contents of mice with the indicated genotypes at 5 weeks of age. n = 3 for each genotype. *P < 0.05.

(D) Hematoxylin-eosin staining of sections showing representative islets from mice with the indicated genotypes at 5 weeks of age. Bars, 50 μm.

(E) Pancreatic insulin contents of wild-type (n = 8), *Eif4ebp1*$^{-/-}$ (n = 4), *Wfs1*$^{-/-}$ (n = 15)

and *Eif4ebp1*$^{-/-}$*Wfs1*$^{-/-}$ (n = 12) mice at 27-30 weeks of age. **P < 0.01.

(F) Insulin positive areas in pancreatic sections of wild-type (n = 3), *Eif4ebp1*$^{-/-}$ (n = 3), *Wfs1*$^{-/-}$ (n = 4) and *Eif4ebp1*$^{-/-}$*Wfs1*$^{-/-}$ (n = 5) mice at 27-30 weeks of age. *P < 0.05.

(G) [^{35}S]methionine/cysteine incorporation in islets with indicated genotypes at 5-6 weeks of age. Ten % of lysates were also probed with an anti-actin antibody. A representative autoradiogram is shown in the left. Lane 1, wild-type; 2, *Eif4ebp1*$^{-/-}$; 3, *Ins2*$^{WT/C96Y}$; 4, *Eif4ebp1*$^{-/-}$*Ins2*$^{WT/C96Y}$. Data from 4 experiments are summarized in the right. *P < 0.05.

(H) [^{35}S]Met/Cys-labeling as in (G) in islets with the indicated genotypes at 6-8 weeks of age. Lane 1, wild-type; 2, *Eif4ebp1*$^{-/-}$; 3, *Wfs1*$^{-/-}$; 4, *Eif4ebp1*$^{-/-}$*Wfs1*$^{-/-}$. Data from 3 experiments are summarized in the right panel. *P < 0.05.

Error bars represent SEM.

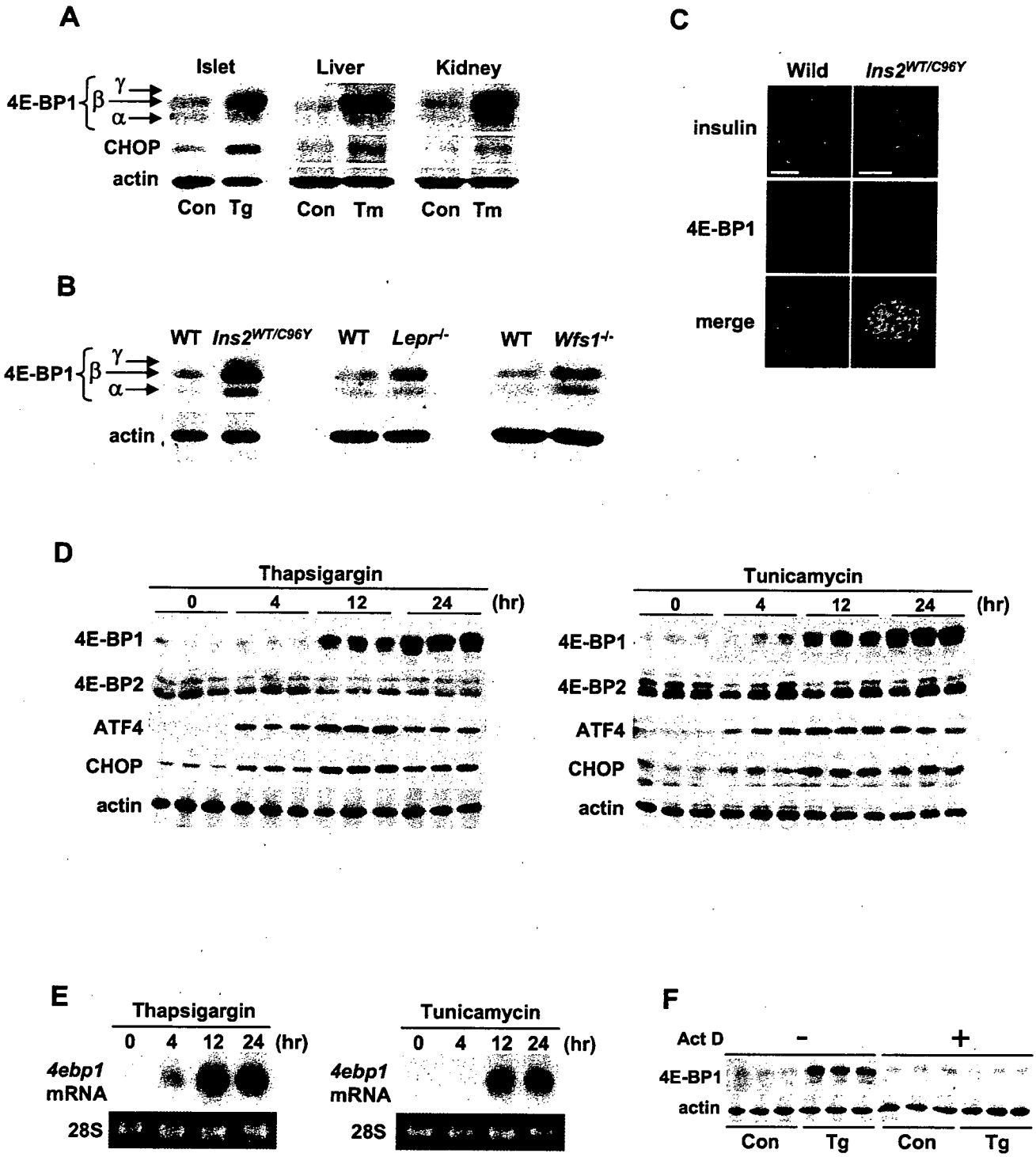
A
Islet
Liver
Kidney
4E-BP1
β
γ
α
CHOP
actin
Con Tg
Con Tm
Con Tm
B
WT Ins2WT/C96Y
WT Lepr-/-
WT Wfs1-/-
4E-BP1
β
γ
α
actin
C
Wild
Ins2WT/C96Y
insulin
4E-BP1
merge
D
Thapsigargin
0 4 12 24 (hr)
4E-BP1
4E-BP2
ATF4
CHOP
actin
Tunicamycin
0 4 12 24 (hr)
4E-BP1
4E-BP2
ATF4
CHOP
actin
E
Thapsigargin
0 4 12 24 (hr)
4ebp1 mRNA
28S
Tunicamycin
0 4 12 24 (hr)
4ebp1 mRNA
28S
F
Act D
-
+
4E-BP1
actin
Con Tg Con Tg

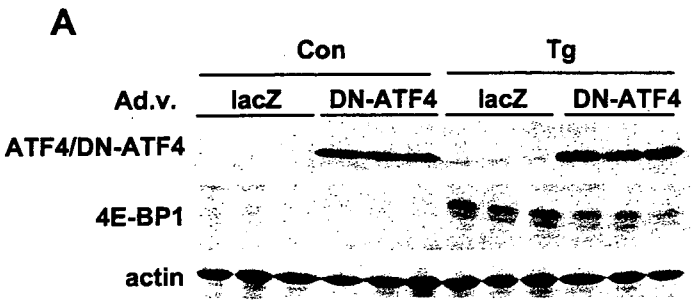
A
Con
Tg
Ad.v.
lacZ
DN-ATF4
lacZ
DN-ATF4
ATF4/DN-ATF4
4E-BP1
actin

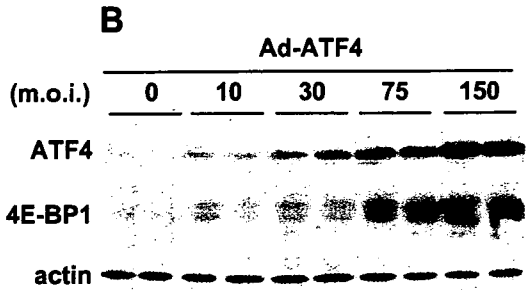
B
Ad-ATF4
(m.o.i.)
0
10
30
75
150
ATF4
4E-BP1
actin

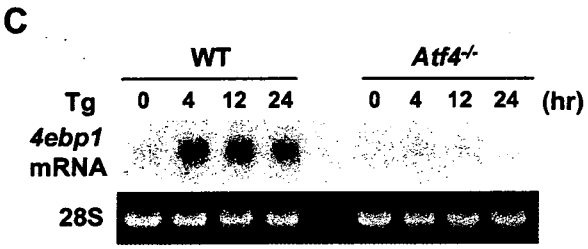
C
WT
Atf4-/-
Tg
0 4 12 24
0 4 12 24
(hr)
4ebp1
mRNA
28S

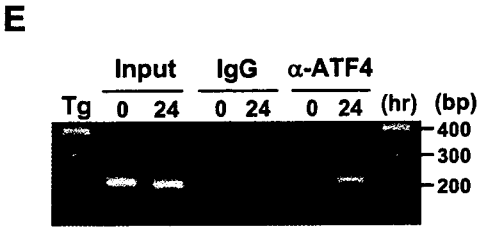
E
Input
IgG
α-ATF4
Tg
0 24
0 24
0 24
(hr)
(bp)
400
300
200

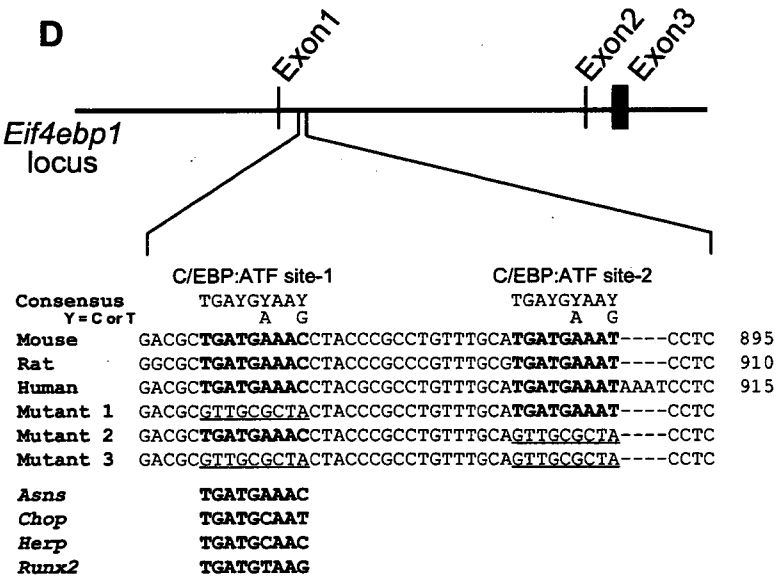
D
Exon1
Exon2
Exon3
Eif4ebp1
locus
C/EBP:ATF site-1
C/EBP:ATF site-2
Consensus
Y=C or T
TGAYGYAAY
A G
TGAYGYAAY
A G
Mouse GACGCTGATGAAACCTACCCGCCTGTTTGCATGATGAAAT----CCTC 895
Rat GGCGCTGATGAAACCTACCCGCCCGTTTGCGTGATGAAAT----CCTC 910
Human GACGCTGATGAAACCTACGCGCCTGTTTGCATGATGAAATAAATCCTC 915
Mutant 1 GACGCGTTGCGCTACTACCCGCCTGTTTGCATGATGAAAT----CCTC
Mutant 2 GACGCTGATGAAACCTACCCGCCTGTTTGCAGTTGCGCTA----CCTC
Mutant 3 GACGCGTTGCGCTACTACCCGCCTGTTTGCAGTTGCGCTA----CCTC
Asns TGATGAAAC
Chop TGATGCAAT
Herp TGATGCAAC
Runx2 TGATGTAAG

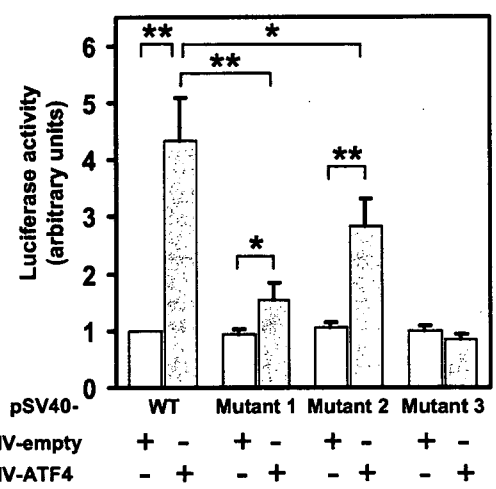
F
Luciferase activity
(arbitrary units)
0
1
2
3
4
5
6
**
*
**
*
**
pSV40-
WT
Mutant 1
Mutant 2
Mutant 3
pCMV-empty
pCMV-ATF4

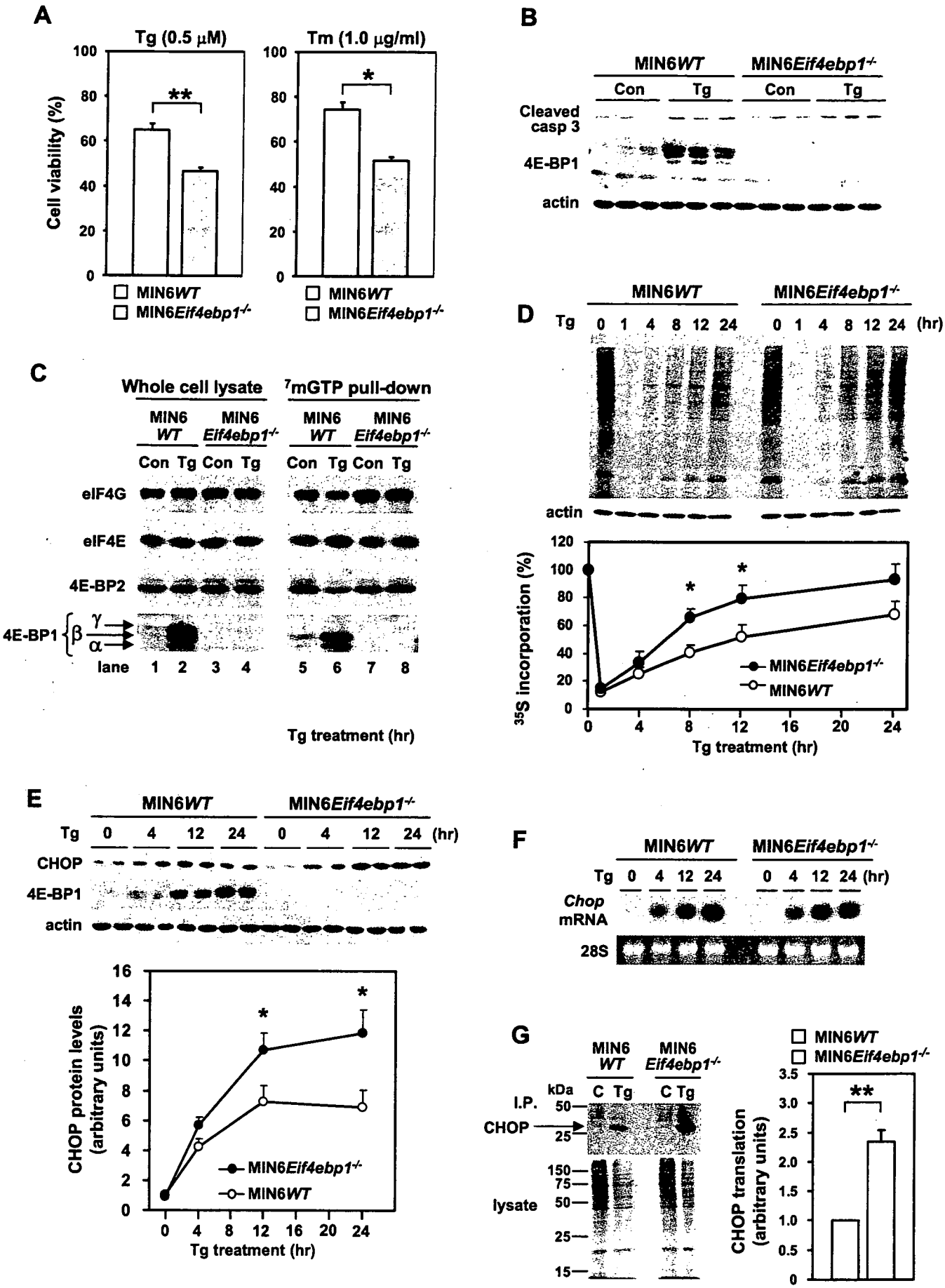
A
Tg (0.5 μM)
Tm (1.0 μg/ml)
Cell viability (%)
MIN6WT
MIN6Eif4ebp1-/-
B
MIN6WT
MIN6Eif4ebp1-/-
Con
Tg
Cleaved casp 3
4E-BP1
actin
C
Whole cell lysate
7mGTP pull-down
MIN6 WT
MIN6 Eif4ebp1-/-
Con Tg Con Tg
eIF4G
eIF4E
4E-BP2
4E-BP1
γ
β
α
lane 1 2 3 4 5 6 7 8
Tg treatment (hr)
D
Tg 0 1 4 8 12 24 0 1 4 8 12 24 (hr)
actin
35S incorporation (%)
Tg treatment (hr)
E
Tg 0 4 12 24 0 4 12 24 (hr)
CHOP
4E-BP1
actin
CHOP protein levels (arbitrary units)
Tg treatment (hr)
F
Tg 0 4 12 24 0 4 12 24 (hr)
Chop mRNA
28S
G
MIN6 WT
MIN6 Eif4ebp1-/-
C Tg C Tg
kDa
I.P.
CHOP
lysate
CHOP translation (arbitrary units)

Yamaguchi *et al.* Figure 4

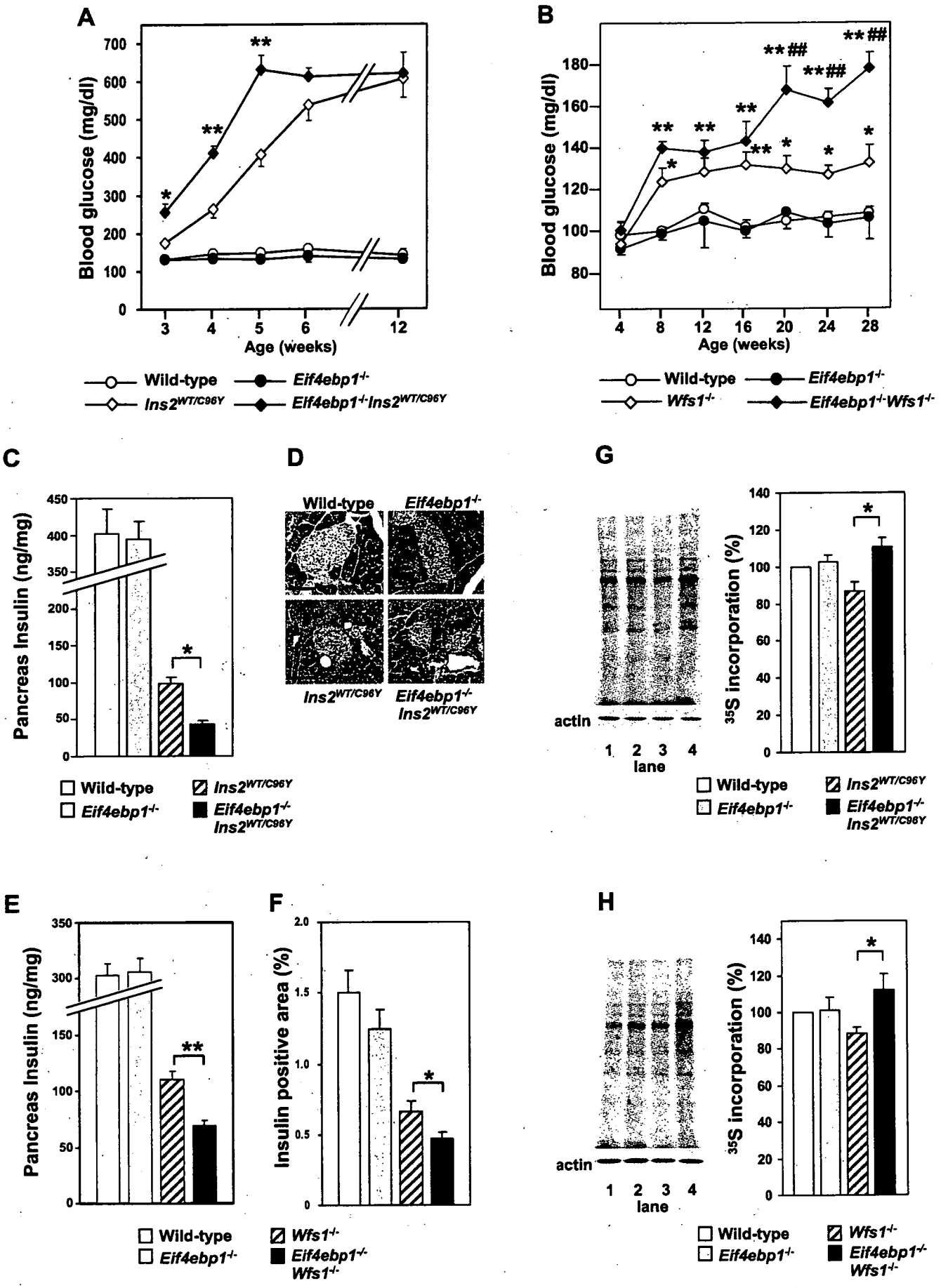

Supplemental Data

ATF4-Mediated Induction of 4E-BP1 Contributes to Pancreatic β Cell Survival under Endoplasmic Reticulum Stress

Suguru Yamaguchi, Hisamitsu Ishihara, Takahiro Yamada, Akira Tamura, Masahiro Usui, Ryu Tominaga, Yuichiro Munakata, Chihiro Satake, Hideki Katagiri, Fumi Tashiro, Hiroyuki Aburatani, Kyoko Tsukiyama-Kohara, Jun-ichi Miyazaki, Nahum Sonenberg and Yoshitomo Oka

Supplemental Figures

Figure S1

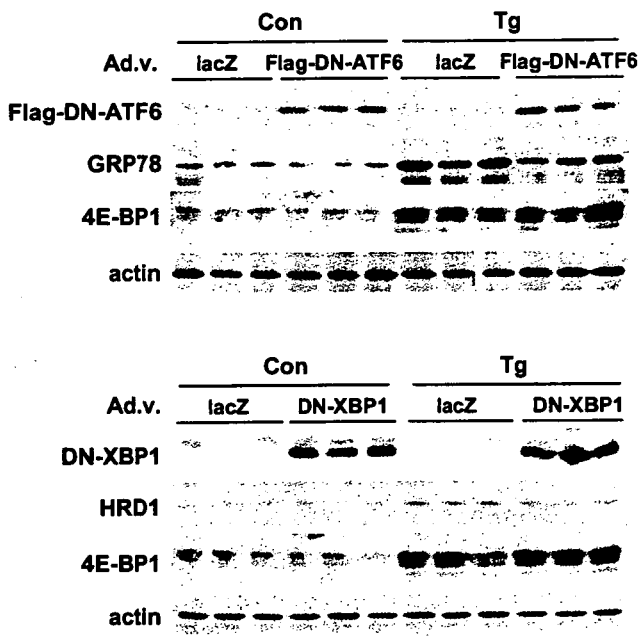

Figure S1. Effects of DN-ATF or DN-XBP1 expression on 4E-BP1 induction

Upper panel: no suppression of thapsigargin-triggered 4E-BP1 induction with expression of the Flag-tagged dominant-negative (DN) ATF6 (Flag-DN-ATF6: ATF6(171-373) lacking the activation domain (Yoshida et al., 2000)). MIN6 cells infected with an adenovirus expressing either lacZ or the Flag-DN-ATF6 were treated with vehicle (0.05% DMSO) control (Con) or thapsigargin (Tg, 0.5 μM) for 12 hr. Cell lysates were analyzed for expressions of Flag-DN-ATF6, GRP78 (ATF6-target), 4E-BP1 and actin (loading control).

Lower panel: no suppression of Tg-triggered 4E-BP1 induction with expression of the DN-XBP1 (XBP1(1-188) lacking the activation domain (Lee et al., 2003)). MIN6 cells infected with an adenovirus expressing either lacZ or the DN-XBP1 were treated with vehicle control (Con) or Tg for 12 hr. Cell lysates were analyzed for expressions of DN-XBP1, HRD1 (XBP1-target), 4E-BP1 and actin (loading control).

Figure S2

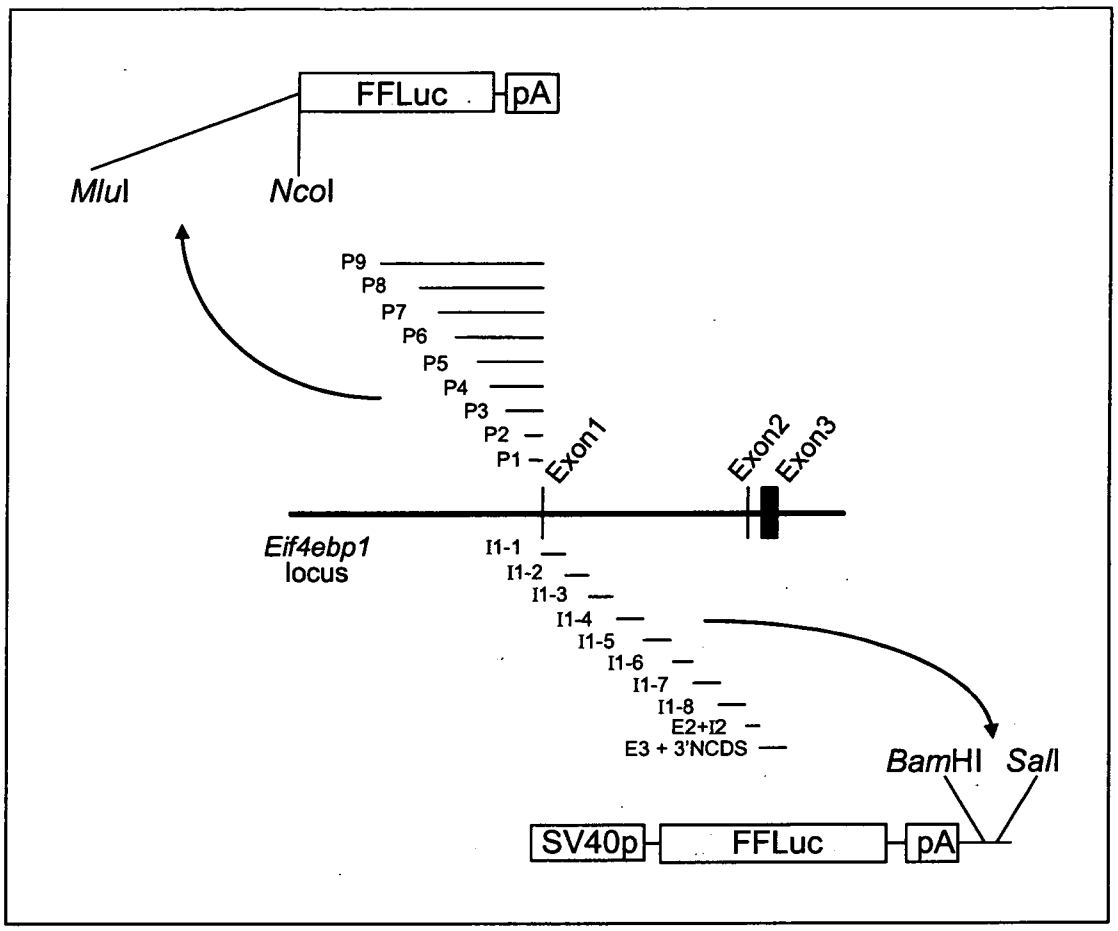
FFLuc
pA
MluI
NcoI
P9
P8
P7
P6
P5
P4
P3
P2
P1
Exon1
Exon2
Exon3
Eif4ebp1
locus
I1-1
I1-2
I1-3
I1-4
I1-5
I1-6
I1-7
I1-8
E2+I2
E3 + 3'NCDS
BamHI
SalI
SV40p
FFLuc
pA

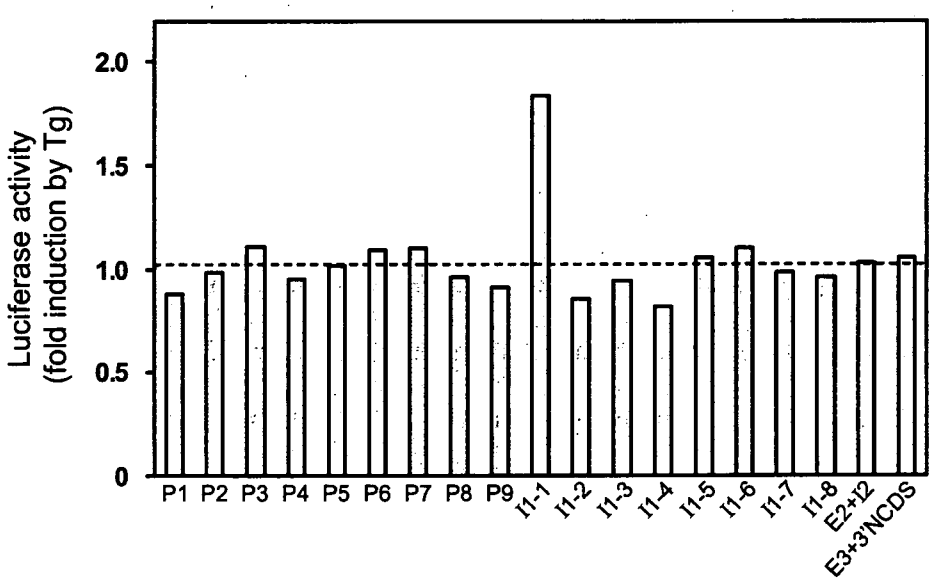
Luciferase activity
(fold induction by Tg)
2.0
1.5
1.0
0.5
0
P1
P2
P3
P4
P5
P6
P7
P8
P9
I1-1
I1-2
I1-3
I1-4
I1-5
I1-6
I1-7
I1-8
E2+I2
E3+3'NCDS

Figure S2. Search for mouse *Eif4ebp1* gene segments conferring Tg-responsiveness to luciferase reporter constructs

Upper panel: reporter constructs used for luciferase activity measurements are presented. PCR-amplified *Eif4ebp1* promoter segments were cloned into the pGL3-basic construct (Promega). P1, -1 to –260 (A in the initial ATG codon is determined as +1); P2, -1 to -1,129; P3, -1 to -2,216; P4, -1 to -3,182; P5, -1 to –4,027; P6, -1 to -4,791; P7, -1 to –6,537; P8, -1 to -7,978; P9, -1 to -9,968. PCR-amplified *Eif4ebp1* segments spanning from exon 1 to the 3' non-coding sequence (3'NCDS) were cloned into the pGL3-promoter construct (Promega). I1-1, +1 to 1,821; I1-2, 1,821 to 3,409; I1-3, 3,409 to 5,198; I1-4, 5,198 to 6,957; I1-5, 6,957 to 8,752; I1-6, 8,752 to 9,977; I1-7, 9,977 to 11,804; I1-8, 11,804 to 12,949; E2+I2, 12,921 to 14,703; E3+3'NCDS, 14,704 to 16,260.

Lower panel: thapsigargin (Tg)-induced firefly luciferase activity in MIN6 cells transfected with reporter constructs shown in the upper panel. Firefly luciferase activity was normalized to Renilla luciferase activity and ratios of normalized activities in the presence to those in the absence of Tg are presented. Each experiment was performed employing 1 or 2 constructs and all data are presented together in one panel. Values are the means of 1 to 3 experiments, each performed in triplicate. Experiments were always conducted with a negative control construct (pGL3-promoter: a *SV40* promoter construct with no insertion between the *Bam*HI and *Sal*I sites) and a positive control construct (pGL3-basic with the *Chop* promoter). Fold inductions of the negative and positive controls were 1.03 ± 0.09 and 3.04 ± 0.11-fold (n = 25), respectively. Data obtained with the negative control are shown as a dashed line.

Figure S3

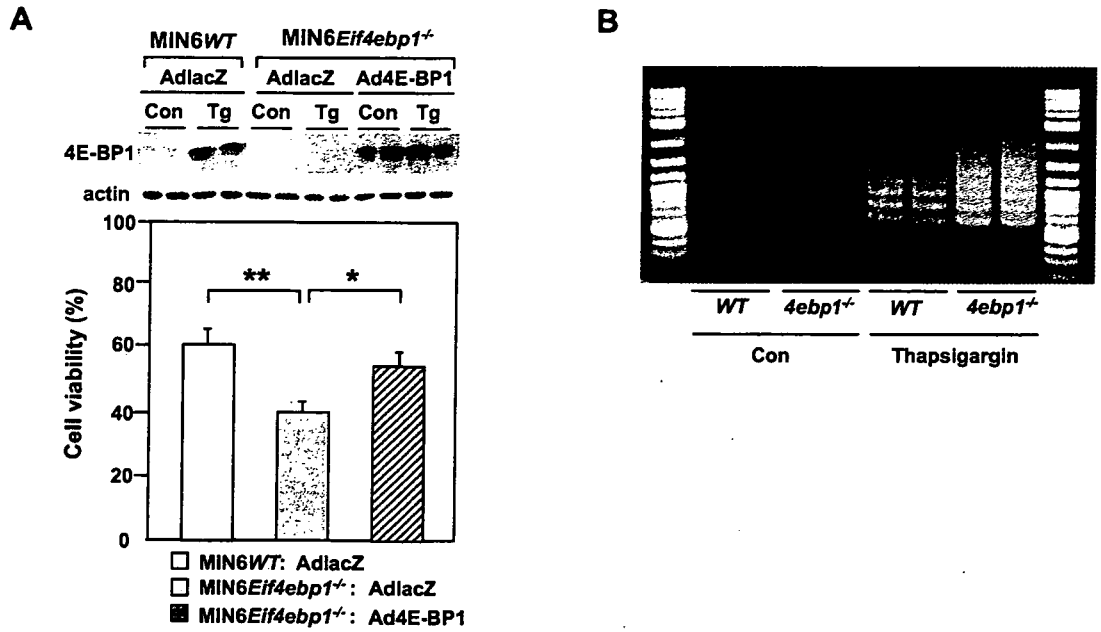

Figure S3. Higher sensitivity of 4E-BP1-deficient MIN6 cells and islets to ER stress

(A) Reduced viability of MIN6*Eif4ebp1*$^{-/-}$ cells treated with 0.5 μM thapsigargin (Tg) was restored by re-expression of 4E-BP1. Data from MIN6*WT* cells treated with vehicle (0.05% DMSO) were taken as 100%. Error bars show SEM. n = 4; *P < 0.05, **P < 0.01. Adenovirus-mediated re-expression of 4E-BP1 is shown in the upper panel. Con, vehicle-treated cells.

(B) Increased apoptotic DNA ladder formation in isolated islets from *Eif4ebp1*$^{-/-}$ mice. Islets isolated from mice of each genotype at 12 weeks of age were incubated in RPMI medium for 3 days and DNA fragmentation was analyzed by ligation-mediated PCR as described previously (Ishihara et al., 2004).

Figure S4

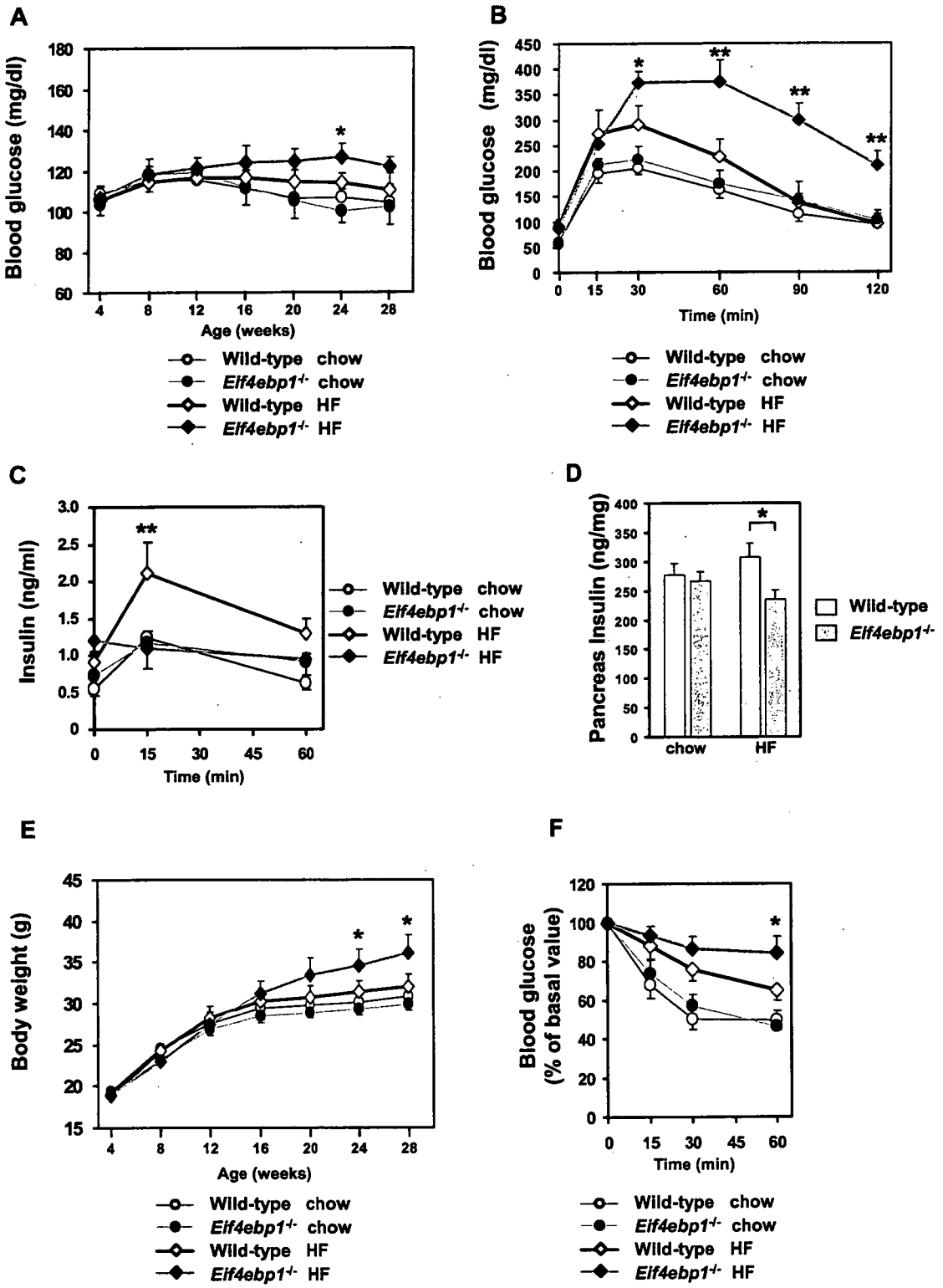
A
Blood glucose (mg/dl)
Age (weeks)
Wild-type chow
Elf4ebp1-/- chow
Wild-type HF
Elf4ebp1-/- HF
B
Blood glucose (mg/dl)
Time (min)
Wild-type chow
Elf4ebp1-/- chow
Wild-type HF
Elf4ebp1-/- HF
C
Insulin (ng/ml)
Time (min)
Wild-type chow
Elf4ebp1-/- chow
Wild-type HF
Elf4ebp1-/- HF
D
Pancreas Insulin (ng/mg)
chow
HF
Wild-type
Elf4ebp1-/-
E
Body weight (g)
Age (weeks)
Wild-type chow
Elf4ebp1-/- chow
Wild-type HF
Elf4ebp1-/- HF
F
Blood glucose (% of basal value)
Time (min)
Wild-type chow
Elf4ebp1-/- chow
Wild-type HF
Elf4ebp1-/- HF

Figure S4. Body weight and glucose homeostasis in wild-type and *Eif4ebp*$^{-/-}$ mice fed standard chow or a high fat diet (HFD)

(A) Fed blood glucose levels of wild-type and *Eif4ebp*$^{-/-}$ mice on standard chow or a HFD (Research Diets D12451).

(B) Blood glucose levels during intraperitoneal glucose tolerance tests (2 g glucose per kg of body weight) in wild-type and *Eif4ebp*$^{-/-}$ mice fed chow or a HFD at 24 weeks of age.

(C) Plasma insulin levels during intraperitoneal glucose tolerance tests (2 g glucose per kg of body weight) in wild-type and *Eif4ebp*$^{-/-}$ mice fed chow or a HFD at 26 weeks of age.

(D) Pancreatic insulin contents of wild-type and *Eif4ebp*$^{-/-}$ mice fed chow or a HFD at 28 weeks of age.

(E) Growth curves of wild-type and *Eif4ebp*$^{-/-}$ mice fed chow or a HFD.

(F) Insulin tolerance tests in wild-type and *Eif4ebp*$^{-/-}$ mice fed chow or a HFD at 25 weeks of age. After a 6 hr fast, mice were given an intraperitoneal injection of insulin (0.75 μU/g body weight). Blood glucose levels at time zero were 69 ± 5 (chow-fed wild-type), 84 ± 11 (chow-fed *Eif4ebp1*$^{-/-}$), 79 ± 5 (HFD-fed wild-type) and 107 ± 6 mg/dl (HFD-fed *Eif4ebp1*$^{-/-}$).

*$P < 0.05$ and **$P < 0.01$, between HFD-fed *Eif4ebp*$^{-/-}$ and HFD-fed wild-type mice. n = 4-6.

Error bars show SEM.

Figure S5

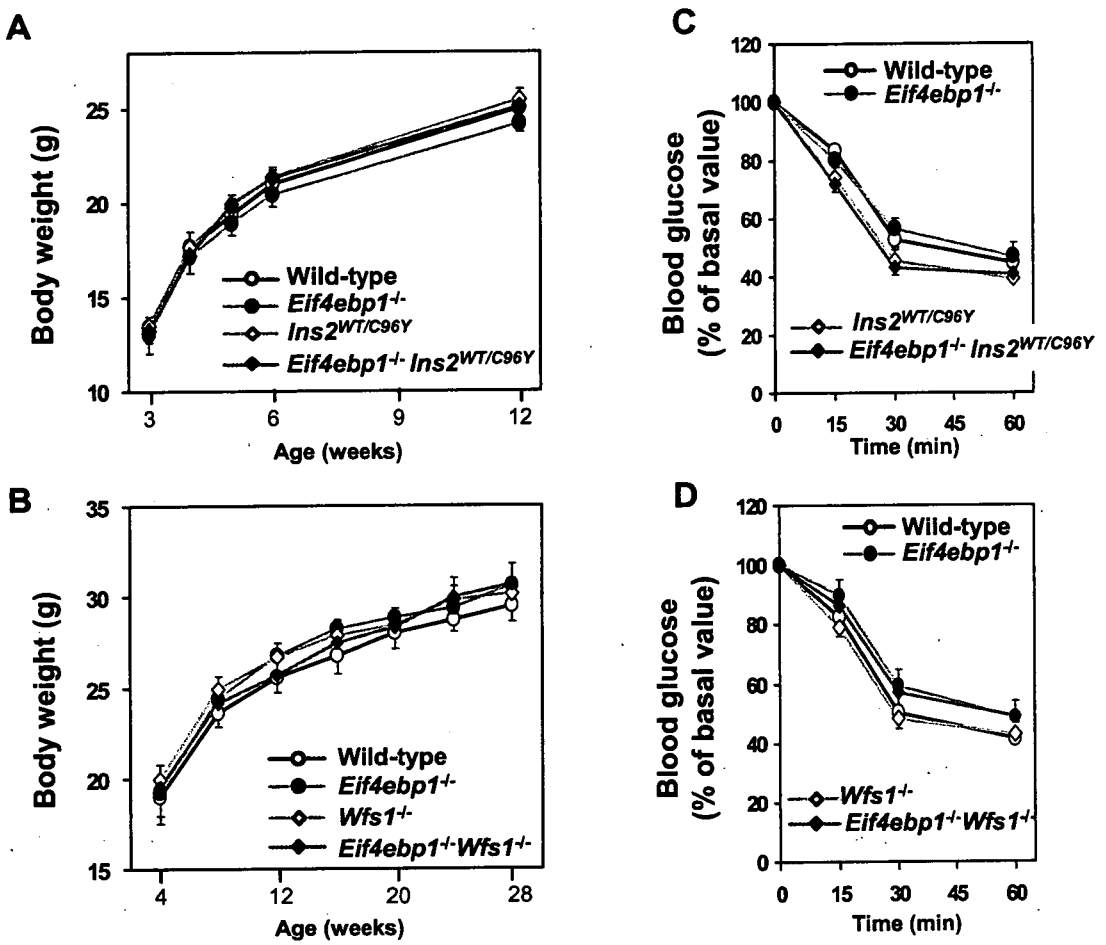

Figure S5. Characterization of 4E-BP1-deficient *Ins2*$^{WT/C96Y}$ and 4E-BP1-deficient *Wfs1*$^{-/-}$ mice

(A) Growth curves of wild-type, *Eif4ebp*$^{-/-}$, *Ins2*$^{WT/C96Y}$ and *Eif4ebp1*$^{-/-}$*Ins2*$^{WT/C96Y}$ mice. n = 5-11.

(B) Growth curves of wild-type, *Eif4ebp1*$^{-/-}$, *Wfs1*$^{-/-}$ and *Eif4ebp1*$^{-/-}$*Wfs1*$^{-/-}$ mice. n = 8-15.

(C) Intraperitoneal insulin tolerance tests in wild-type, *Eif4ebp1*$^{-/-}$, *Ins2*$^{WT/C96Y}$ and *Eif4ebp1*$^{-/-}$*Ins2*$^{WT/C96Y}$ mice at 5 weeks of age. After a 6 hr fast, mice were given an

intraperitoneal injection of insulin (0.75 μU/g body weight). Blood glucose levels at time zero were 77 ± 6 (wild-type), 72 ± 5 (*Eif4ebp1*$^{-/-}$), 216 ± 19 (*Ins2*$^{WT/C96Y}$) and 271 ± 23 mg/dl (*Eif4ebp1*$^{-/-}$*Ins2*$^{WT/C96Y}$). n = 5-8. Insulin sensitivities did not differ among the four groups.

(D) Insulin tolerance tests in wild-type, *Eif4ebp1*$^{-/-}$, *Wfs1*$^{-/-}$ and *Eif4ebp1*$^{-/-}$*Wfs1*$^{-/-}$ mice at 24 weeks of age. After a 6 hr fast (time zero), blood glucose was reduced to similar levels in all four groups; blood glucose levels at time zero were 79 ± 6 (wild-type), 73 ± 5 (*Eif4ebp1*$^{-/-}$), 80 ± 7 (*Wfs1*$^{-/-}$) and 77 ± 9 mg/dl (*Eif4ebp1*$^{-/-}$*Wfs1*$^{-/-}$), n = 7-9. Insulin sensitivities did not differ among the four groups ($P > 0.094$).

Error bars show SEM.

Figure S6

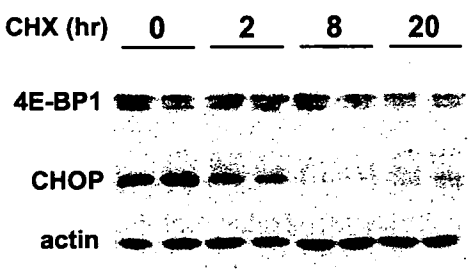

Figure S6. 4E-BP1 protein is stable within cells

MIN6 cells were incubated with thapsigargin (0.5 μM) for 24 hr, washed with PBS and treated with cycloheximide (CHX, 50 μM) for the indicated period. Cell lysates were subjected to immunoblotting with an anti-4E-BP1 antibody. Immunoblotting results for CHOP are also presented for comparison. The data are representative of three independent experiments.

Supplemental References

Lee, A.-H., Iwakoshi, N.N., and Glimcher, L.H. (2003). XBP-1 regulates a subset of endoplasmic reticulum resident chaperone genes in the unfolded protein response. Mol. Cell. Biol. 2003. *23*, 7448-7459.

Yoshida, H., Okada, T., Haze, K., Yanagi, H., Yura, T., Negishi, M., and Mori, K. (2000). ATF6 activated by proteolysis binds in the presence of NF-Y (CBF) directly to the cis-acting element responsible for the mammalian unfolded protein response. Mol. Cell. Biol. *20*, 6755-6767.

J Gastroenterol 2007; 42:411–423
DOI 10.1007/s00535-007-2030-3

Journal of Gastroenterology

Review

Molecular biology of hepatitis C virus

Tetsuro Suzuki, Hideki Aizaki, Kyoko Murakami, Ikuo Shoji, and Takaji Wakita

Department of Virology II, National Institute of Infectious Diseases, 1-23-1 Toyama, Shinjuku-ku, Tokyo 162-8640, Japan

Infection with hepatitis C virus (HCV), which is distributed worldwide, often becomes persistent, causing chronic hepatitis, cirrhosis, and hepatocellular carcinoma. For many years, the characterization of the HCV genome and its products has been done by heterologous expression systems because of the lack of a productive cell culture system. The development of the HCV replicon system is a highlight of HCV research and has allowed examination of the viral RNA replication in cell culture. Recently, a robust system for production of recombinant infectious HCV has been established, and classical virological techniques are now able to be applied to HCV. This development of reverse genetics-based experimental tools in HCV research can bring a greater understanding of the viral life cycle and pathogenesis of HCV-induced diseases. This review summarizes the current knowledge of cell culture systems for HCV research and recent advances in the investigation of the molecular virology of HCV.

Key words: hepatitis C virus, translation, polyprotein processing, RNA replication, viral assembly, ubiquitin

Introduction

Hepatitis C virus (HCV), discovered in 1989, is a major etiologic agent of posttransfusion- and sporadic non-A, non-B hepatitis[1] and at present infects approximately 200 million people worldwide.[2,3] Persistent infection with HCV is associated with the development of chronic hepatitis, hepatic steatosis, cirrhosis, and hepatocellular carcinoma.[3,4–8] HCV is a small, enveloped RNA virus that belongs to the *Hepacivirus* genus of the *Flaviviridae* family.[9,10] Its genome consists of a single-strand of positive-sense RNA of approximately 9.6kb, which contains an open reading frame (ORF) coding for a polyprotein precursor of approximately 3000 residues.[11] The precursor is cleaved into at least ten different proteins: the structural proteins core, E1, E2, and p7, and the nonstructural proteins NS2, NS3, NS4A, NS4B, NS5A, and NS5B (Fig. 1).

To date, six major genotypes of HCV have been identified that differ by 31%–34% in their nucleotide sequence and by about 30% in their amino acid sequence. It has been shown that HCV, like many other RNA viruses, circulates in infected individuals as a population of diverse but closely related variants referred to as quasispecies.[12] This quasispecies model of mixed virus populations may confer a significant survival advantage, because the simultaneous presence of multiple variant genomes and the high rate of generation of new variants allows rapid selection of mutants better suited to new environmental conditions.[13]

Specific anti-HCV drugs that efficiently block virus production are not yet available. The current standard care is combination therapy with interferon (IFN)-α and the nucleoside analog ribavirin, which cures about 40% of hepatitis C patients infected by HCV genotype 1, the most prevalent genotype in industrialized countries, and about 80% of those infected by genotype 2 or 3.[14,15] Since many patients still do not benefit from the treatment and IFN therapy is associated with undesirable side effects such as headache, fever, severe depression, myalgia, arthralgia, and hemolytic anemia, development of innovative treatment alternatives for hepatitis C patients is immediately needed. Studies of HCV life cycle in cell cultures have been greatly facilitated by the development of genetically engineered viral genomes that are capable of self-amplifying to high levels (replicon system), and by recent establishment of a production system for recombinant infectious HCV. Such progress will aid in the development of significantly improved HCV antiviral agents.

Received: February 8, 2007 / Accepted: February 10, 2007
Reprint requests to: T. Suzuki

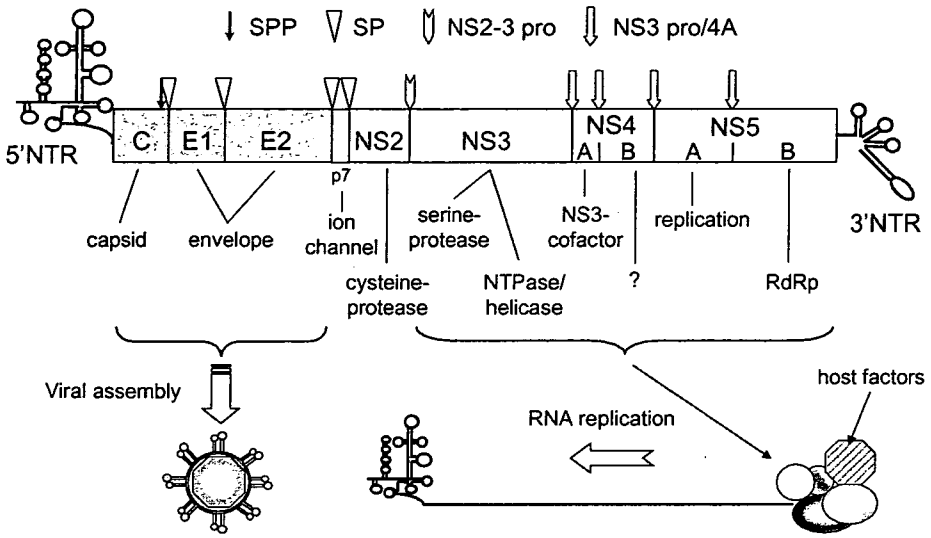

Fig. 1. Hepatitis C virus (HCV) genome organization and polyprotein processing. Posttranslational cleavages by signal peptide peptidase (*SPP*), signal peptidase (*SP*), NS2–NS3 protease (*NS2–3 pro*), and NS3 protease and NS4A complex (*NS3 pro/4A*) lead to the production of functional HCV proteins. *NTR*, nontranslated region

Cell culture systems for HCV research

Although substantial information on HCV protein structure and function has been obtained from the use of a variety of cell culture and in vitro expression systems, for many years, HCV research has been hampered by the restricted host range and the inefficiency of cell culture models for viral infection and propagation. The development of the HCV replicon system, therefore, is a milestone in HCV research and has allowed examination of viral RNA replication in cell culture.[16] Expression systems of heterologous virus genes based on RNA replicons have been established in a variety of positive-strand RNA viruses such as polio virus,[17–20] the alphavirus Semliki Forest virus,[21] Sindbis virus,[22–25] Kunjin virus,[26] human rhinovirus 14,[27] and bovine viral diarrhea virus.[28] In general, advantages of replicon systems are (1) a high level of gene expression and RNA replication, (2) easy construction of recombinants, and (3) a wide permissible host range.

The HCV replicons are typically composed of selectable, bicistronic RNA, with the first cistron containing the HCV 5′ nontranslated region (NTR), which directs translation of the gene encoding the neomycin phosphotransferase, and the second cistron containing the internal ribosome entry site (IRES) of the encephalomyocarditis virus, which directs translation of HCV NS3 through NS5B region, and the 3′ NTR. The prototype subgenomic replicon utilized a particular HCV genotype 1b clone termed Con1. Following transfection of RNA generated by in vitro transcription of the cloned replicon sequences into a human hepatoma cell line Huh-7, antibiotic G418-resistant cells could be obtained in which the subgenomic RNA replicated autonomously. RNA replication was first detected at relatively low frequency, followed by the identification of replicons harboring cell culture-adaptive mutations, which increased the efficiency of replication initiation by several orders of magnitude.[29–31]

Adaptive mutations were found primarily at the N-terminus of the NS3 helicase, in NS4B, and in the center of NS5A, which is upstream of the region putatively involved in IFN sensitivity. Most of the mutations in NS5A are located at highly conserved serine residues and lead to change in the phosphorylation state of NS5A.[32,33] A combination of adaptive mutation in NS3 and NS5A resulted in the highest level of replication of a particular HCV genotype 1b isolate.[31] Later work, however, has indicated that adaptive mutations can arise in most of the viral nonstructural proteins.[34,35] The mechanisms by which adaptive mutations increase RNA replication efficiency are not well understood.

In the last 7 years, a variety of different replicons have been generated, including replicons with reporters or markers such as luciferase and green fluorescent protein, replicons from genotype 1a and 2a, and genome-length dicistronic HCV RNAs (genomic HCV replicons). HCV replicons with reporter genes allow us to execute fast and reproducible screening of large series of compounds for antivirals.[36–38] Huh-7 cells are the most permissive for HCV replicons. However, variability in the permissiveness for replicons has been observed for a given Huh-7 cell pool, and the cells that are able to support efficient replication of the viral genome are enriched during selection such as G418 treatment. A so-called "cured" cell clone, which can be prepared by removing the replicons by treatment with IFN, supports viral replication to a much higher level in many cases and is useful for introducing genome-length HCV RNAs.[39,40]

An HCV genotype 2a replicon with the JFH-1 strain, which was first isolated from the serum of a Japanese patient with fulminant hepatitis C by our group,[41] replicates efficiently in not only Huh-7 cells but also other